

# Solvent concentration in a specified region of regenerated cellulose solid evaluated from dynamic viscoelasticity in a hydrophilic solvent

Sei-ichi Manabe\*, Rumiko Fujioka

*Fukuoka Women's University, 1-1-1 Kasumigaoka, Higashi-ku, Fukuoka 813-8529, Japan*

Received 19 January 1999; accepted 10 May 1999

## Abstract

An attempt was made to evaluate the solvent concentration  $\nu$  in a specified amorphous region by the use of semi-empirical equation

$$\nu = (1 - T_{fc}/T_f)/(2T_{fc}/T_{m(s)} - T_{fc}/T_f)$$

where  $T_{fc}$  and  $T_f$  are peak temperatures of a dynamic loss tangent  $\tan \delta$  of a given dynamic absorption in solvent and dry air, respectively, and  $T_{m(s)}$  is the melting point of the solvent. A polymer blend with polystyrene and polymethylmethacrylate was used to confirm the reliability of the equation. The well-characterized two cuprammonium regenerated cellulose fibers, which were composed of the primary particles having ca. 15 nm in size, were used. More than 20 solvents with –OH groups were selected as an immersing media in order to clarify the diffusibility of a solvent into an amorphous region. The isochronal viscoelasticity in a solvent was measured. The results were: (1) the reliability of the equation was confirmed; (2) the  $\nu$  value of the region relating to the dynamic absorption observed at higher temperature was smaller than that at lower temperature; (3) as for the interfacial region of the primary particle,  $\nu$  ranged between 0.05 and 0.30 and varied depending on the chemical structure of a solvent. The  $\nu$  value increased with a decrease in a molecular weight MW of the solvent and showed a minimum value at the solvent, which showed the critical balance between hydrophilic and lipophilic properties; (4) as for the inside of the primary particle,  $\nu$  ranged between 0 and 0.21 and decreased with an increase in MW. With an increase in the number of OH groups in a solvent,  $\nu$  increased. We concluded that the solvent diffused into a specific amorphous region depending on its affinity to cellulose molecule and the molecular size and the  $\nu$  value was evaluated through the peak temperature of  $\tan \delta$  measured in the solvent. © 2000 Elsevier Science Ltd. All rights reserved.

**Keywords:** Regenerated cellulose; Dynamic viscoelasticity; Amorphous region; Hydrophilic solvent; Dynamic loss tangent; Free volume

## 1. Introduction

The detailed description about the aggregation structure of the cellulose chains in an amorphous region for both solids of natural and regenerated cellulose (referred to as cellulose without distinguishing both kinds of cellulose) has not yet been given. The ambiguous description may be due to the difficulty in preparation of the amorphous solid and the lack of appropriate methods for evaluation of chain aggregation state. Because of the complexity of the aggregation state there remain many confusions in the past studies about the glass transition temperature ( $T_g$ ) of a cellulose solid. The  $T_g$  ranges between 243 and 423 K in the past data obtained through dilatometry and differential scanning calorimetry (DSC) (Hatakeyama & Kanetsuna, 1969; Haughton & Sellen, 1973; Kamide & Saito, 1985; Klotnikov, Mikhailov & Rayavee, 1977; Kubat & Pattyramie,

1967; Nakamura, 1956, 1957; Ramiah & Goring, 1965; Webba & Asiz, 1962). We have proposed the evaluation method of the distribution function of the packing density of the molecular chain in a polymer solid through the isochronal temperature dependence of a dynamic loss tangent ( $\tan \delta$ ) (Manabe & Kamide, 1984; Manabe, Kamide, Nakayama & Kobayashi, 1977). In applying this method to a cellulose solid the molecular mechanism to give  $\tan \delta$  should be given in advance. The molecular motion named as  $\alpha_a$  absorption originates from the segmental micro-Brownian motion of a main chain in an amorphous region.

There have been observed seven dynamic absorptions in the temperature range between 150 and 600 K for a regenerated cellulose solid, such as  $\alpha_1$ ,  $\alpha_{21}$ ,  $\alpha_{22}$ ,  $\alpha_{sh}$ ,  $\alpha_{H_2O}$ ,  $\beta_{a1}$  and  $\beta_{a2}$  from the higher temperature side (Manabe & Fujioka, 1996; Manabe, Iwata & Kamide, 1986). The symbol of  $\alpha$  indicates that the motion is related to the  $\alpha_a$  absorption. In the case of natural cellulose solid (for example, cotton), the separation of these absorptions was not

\* Corresponding author. Tel.: + 81-92-661-2411; fax: + 81-92-661-2415.

clear (Manabe & Fujioka, 1998a). The peak temperature of  $\tan \delta$  measured at 110 Hz in the frequency  $T_{\max}$ , an apparent activation energy of an absorption ( $\Delta H_a$ ), and the absorption mechanism are summarized as follows (Manabe & Fujioka, 1996; Manabe et al., 1986):

- $\alpha_1$ :  $T_{\max} = 558\text{--}578$  K,  $\Delta H_a = 1200$  kJ/mol, the micro-Brownian motion of a segment of a cellulose chain in the structural unit. Here, the structural unit is a primary particle with ca. 15 nm in size for a regenerated cellulose solid, and an elementary micro-fibril with ca. 8 nm in diameter for a natural cellulose solid.
- $\alpha_{21}$ :  $T_{\max} = 488\text{--}563$  K,  $\Delta H_a = 290$  kJ/mol, the micro-Brownian motion of a segment of a cellulose chain in a primary particle.
- $\alpha_{22}$ :  $T_{\max} = 413\text{--}513$  K,  $\Delta H_a = 210$  kJ/mol, the micro-Brownian motion of a segment of a cellulose chain in a primary particle. The distinction of  $\alpha_1$ ,  $\alpha_{21}$  and  $\alpha_{22}$  absorptions originates from the difference in the circumstance of the segments.
- $\alpha_{sh}$ :  $T_{\max} = 388\text{--}477$  K,  $\Delta H_a$  has not been determined yet, the micro-Brownian motion of a segment of a cellulose chain in an interfacial surface region of a primary particle.
- $\alpha_{H_2O}$ :  $T_{\max} = 303\text{--}323$  K,  $\Delta H_a$  has not been determined yet, the cooperative motion of a segment in a primary particle and a water molecule absorbed.
- $\beta_{a1}$ :  $T_{\max} = 225$  K,  $\Delta H_a = 170$  kJ/mol, the local twisting motion of a main chain in an interfacial region of a primary particle.
- $\beta_{a2}$ :  $T_{\max} = 210$  K,  $\Delta H_a = 210$  kJ/mol, the local twisting motion of a main chain in a primary particle.

The fringed micelle model has been proposed for representing the fine structure of a cellulose solid (Hermans, 1949), especially for a regenerated cellulose solid. The structure concerning to a non-crystalline region is described by the lateral order distribution evaluated through the resistance against chemical reagent treatment. From a morphological investigation of the regenerated cellulose hollow fiber during the preparation from cuprammonium solution, we have proposed the particle aggregation model for the representation of the fine structure of the regenerated cellulose solid (Tsurumi, Osawa, Hirasaki, Yamaguchi, Manabe & Yamashiki, 1990). The structural unit of this model is a primary particle with ca. 15 nm in size and occasionally the particle grows into a secondary particle ranging between 70 and 300 nm in size in the case of slow coagulation process (Kamide & Manabe, 1985; Manabe, Kamata, Iijima & Kamide, 1987). The aggregation state of the cellulose chains in an amorphous region is a very important factor which governs the processability of its finishing through the molecular interaction between small molecule (referred to as solvent) such as affinity and diffusibility.

In this article, we intend to improve the semi-empirical equation proposed in the previous paper (Manabe & Fujioka, 1998b) for the evaluation of the solvent concentration existing in a specified amorphous region of a cellulose

solid and intend to confirm its validity and clarify the characteristic feature of the interaction of the cellulose with solvent having OH groups.

## 2. Theoretical background

We have derived the theoretical equation to give the volume fraction  $v$  of a given solvent in a specified amorphous region as follows (Manabe & Fujioka, 1998b):

$$v/(1-v) = (T_f - T_{fc})/(T_{fc} - T_{f(s)})(\alpha_f/\alpha_{f(s)}) \quad (1)$$

$T_f$ ,  $T_{fc}$  and  $T_{f(s)}$  are the freezing temperature of the thermal motion causing a given dynamic absorption (for example,  $\alpha_a$  absorption) for a polymer solid, a swelled polymer solid with a solvent, and a solvent, respectively. The  $\alpha_f$  and  $\alpha_{f(s)}$  are the thermal expansion coefficients of a free volume of a polymer solid and the solvent, respectively. Eq. (1) was derived under the assumptions that the free volume of a polymer solid swelled with a solvent was calculated by the additivity of each component and that the micro-Brownian motion freezed when the free volume fraction decreased into a critical value. The value of  $T_f$  is closely related to  $T_g$  and is higher than  $T_g$  by about a few tens of degrees. By the use of the empirical relations such as  $\alpha_f/\alpha_{f(s)} = 0.5$  and  $T_{fc}/T_{m(s)} = 0.5$  ( $T_{m(s)}$  is the melting temperature of a solvent) is employed, Eq. (2) was derived (Manabe & Fujioka, 1998b)

$$v = (1 - T_{fc}/T_f) / \{1 + (T_{fc} - T_{m(s)})/T_f\} \quad (2)$$

when the empirical relations of  $\alpha_f/\alpha_{f(s)} = 2/3$  and  $T_{f(s)}/T_{m(s)} = 0.5$  were used,

$$v = (1 - T_{fc}/T_f) / \{1 + 0.5(T_{fc}/T_f) - 0.75(T_{m(s)}/T_f)\} \quad (3)$$

The validation of both equations has not been confirmed yet.

At the glass transition temperature, where  $\alpha_a$  absorption occurs, the iso-free volume state may hold and the relation of  $\alpha_f \cdot T_f = \text{constant}$  ( $\cong 0.113$ ) given by Simha and Boyer (1962) may hold even in the case of a solvent. Then Eq. (1) deforms into Eq. (4).

$$v/(1-v) = (T_f - T_{fc})/(T_{fc} - T_{f(s)})(T_{f(s)}/T_f) \quad (4)$$

when the empirical equation of  $T_{f(s)} = 0.5T_{m(s)}$  is used, Eq. (5) is derived

$$v = \{1 - (T_{fc}/T_f)\} / \{2(T_{fc}/T_{m(s)}) - (T_{fc}/T_f)\} \quad (5)$$

Eq. (5) may be applicable only to the  $\alpha_a$  absorption, and is expected to be more reliable than the cases of Eqs. (2) and (3).

## 3. Experimental

### 3.1. Sample preparation

1. *Cuprammonium regenerated cellulose fibers.* Porous hollow fiber having 40 nm in mean pore size, BMM40,

Table 1  
Structural characteristics of BMM40 and NP

| Sample code                      | BMM40                     | NP                      |
|----------------------------------|---------------------------|-------------------------|
| Cross-sectional view             | Hollow fiber              | Circular fiber          |
| Outer diameter ( $\mu\text{m}$ ) | 350                       | 18                      |
| X-ray crystallinity (%)          | 0–2                       | 54                      |
| Birefringence at center          | 0.0016                    | 0.0382                  |
| Structural unit (shape)          | Primary particle (sphere) | Micro-fibril (cylinder) |
| Size of the unit (nm)            | 15                        | 50                      |
| Mean pore size (nm)              | 40                        | <sup>a</sup>            |

<sup>a</sup> Not determined.

and textile fiber NP were used. The preparation conditions of both fibers were given elsewhere (Manabe et al., 1986). Table 1 summarizes the structural characteristics (Manabe & Fujioka, 1998b). After drying at 298 K in vacuum, the samples were immersed in a given solvent at 298 K for more than 48 h.

2. *Polymer blend film.* The blend of polymethylmethacrylate (PMMA) and polystyrene (PS) were dissolved into benzene with weight ratio of 1:1 and then pored into methanol resulting in coprecipitates. PMMA was a commercially available product manufactured by Mitsubishi rayon, and PS was prepared by emulsion polymerization with viscosity average molecular weight of  $8.9 \times 10^4$ . The precipitates were hot pressed into a film with 0.25 mm in thickness at 425 K. The blend film was placed into a saturated vapor of dioxane or a formic acid at 298 K for several tens of hours in order to absorb the solvents.
3. *Hydrophilic solvent with hydroxy groups.* More than 20 solvents were used as an immersing media for the

regenerated cellulose fiber. All were guaranteed reagents manufactured by Wako Pure Chemical Industries, Japan.

### 3.2. Measurement

The temperature dependence of a dynamic viscoelasticity for a regenerated cellulose fiber in a solvent was measured by the method proposed by us (Manabe et al., 1986) using Rheovibron DDV-II *c* manufactured by Toyo-Boldwin. The sample was immersed in the solvent at 298 K for more than 48 h prior to the measurement. the measuring frequency was 110 Hz and heating rate was 3 K/min. The relative error of  $E'$  was less than 10% and that of  $\tan \delta$  was less than 3%.

The concentration of the solvent in the blend film was evaluated through the change in weight at 298 K. The dynamic viscoelasticity was measured in an air under the same frequency and heating rate to the case of a regenerated cellulose.

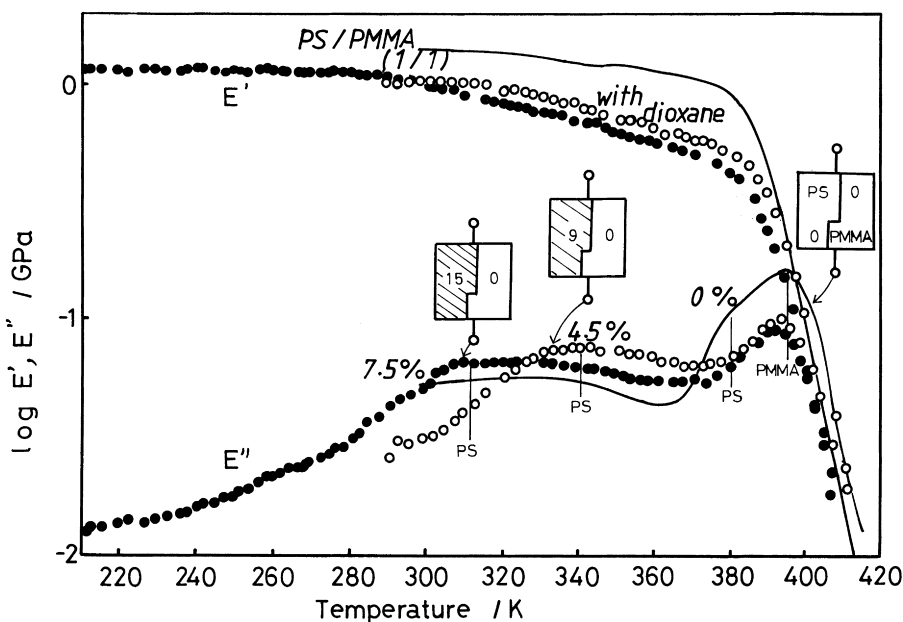


Fig. 1. Temperature dependence of  $E'$  and  $E''$  for blend film of PS and PMMA with weight ratio of 1:1 under coexistence of dioxane. The film was swelled with dioxane and the content was 0, 4.5 and 7.5 wt%.

Table 2

Comparison of solvent concentration  $\nu$  between calculation and preparation for PS/PMMA blend swelled with dioxane

| Component | Preparation | $\nu$ Calculated by |         |         |
|-----------|-------------|---------------------|---------|---------|
|           |             | Eq. (2)             | Eq. (3) | Eq. (5) |
| PMMA      | 0           | 0                   | 0       | 0       |
| PS        | 0.09        | 0.096               | 0.12    | 0.073   |
| PMMA      | 0           | 0                   | 0       | 0       |
| PS        | 0.15        | 0.18                | 0.21    | 0.14    |

Table 3

Comparison of solvent concentration  $\nu$  between calculation and preparation for PS/PMMA blend swelled with formic acid

| Component | Preparation | $\nu$ Calculated by |         |         |
|-----------|-------------|---------------------|---------|---------|
|           |             | Eq. (2)             | Eq. (3) | Eq. (5) |
| PMMA      | 0.18        | 0.19                | 0.24    | 0.15    |
| PS        | 0           | 0                   | 0       | 0       |
| PMMA      | 0.32        | 0.48                | 0.55    | 0.40    |
| PS        | 0           | 0                   | 0       | 0       |

## 4. Results and discussion

### 4.1. Comparison between calculated and prepared values for solvent concentration in an amorphous region

The dispersed state of PS and PMMA in the blend were confirmed to be represented by two separated phase regions, each of which was composed of one component polymer. The size of the region was more than  $0.1\ \mu\text{m}$  in one dimension. Fig. 1 shows the temperature dependence of storage modulus  $E'$  and loss modulus  $E''$  for the blend film of PS and PMMA with the dioxane content of 0, 4.5 and 7.5 wt%. Dioxane is a good solvent for PS and a non-solvent for PMMA. Then, dioxane must dissolve only in the PS phase. The 4.5 wt% dioxane in the blend film indicates that the content in PS is 9.0 wt% and the one in PMMA is 0 wt%. In the case of 7.5 wt% of dioxane, the content in PS phase is regarded as 15 wt%. These reduced contents are cited in the phase representing PS in Takayanagi's model (Takayanagi, Harima & Iwata, 1963). The parameters of  $\lambda$  and  $\phi$  in this model were determined from the value of  $E'$

and  $E''$  so as to fit the observed value to the calculated values by this model. The peak temperature of  $E''$  was regarded as  $T_f$  or  $T_{fc}$  for each component.  $T_f$  values for PS and PMMA were 380 and 396 K, respectively. These values were substituted into Eqs. (2), (3) and (5). Here,  $T_{m(s)}$  of dioxane is 284 K. We evaluated the volume fraction of dioxane  $\nu$  in PS and PMMA regions. Table 2 summarizes the calculated  $\nu$  values for the case of dioxane. Although all calculated values are similar to each other, the values by Eqs. (2) and (3) are larger and that of Eq. (5) is slightly smaller. By comparing with the calculated  $\nu$  and the prepared  $\nu$ , Eq. (5) gives the most reliable value of  $\nu$ .

In Fig. 2 are shown the temperature dependence of  $E'$  and  $E''$  for the blend film swelled with formic acid under the content of 0, 9.0 and 16 wt%. Formic acid is a good solvent for PMMA and a non-solvent for PS. Formic acid exists only in the PMMA phase with the content of 0, 18.0 and 32 wt% for the cases of 0, 9.0 and 16 wt% in a whole film, respectively. In the dynamic equivalent model by Takayanagi, these contents are cited in the PMMA phase. The peak temperature of  $E''$  was determined for each component.  $T_{m(s)}$

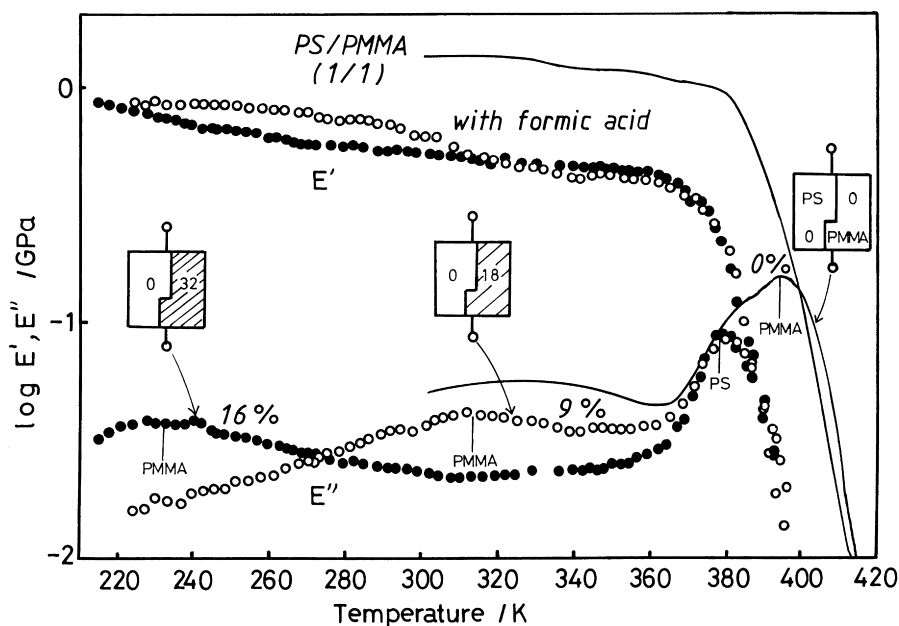


Fig. 2. Temperature dependence of  $E'$  and  $E''$  for blend film of PS and PMMA with weight ratio of 1:1 under coexistence of formic acid. The film was swelled with formic acid and the content was 0, 9.0 and 16 wt%.

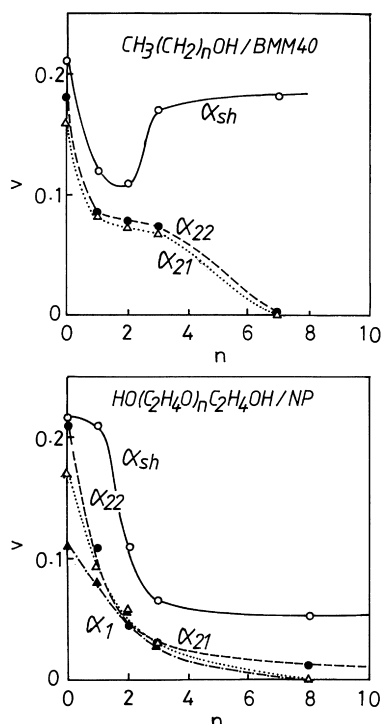


Fig. 3. Solvent content  $v$  in specified amorphous regions for  $n$ -alcohol in BMM40 and for PEG in NP.

of formic acid is 281.4 K. Substituting the temperature into Eqs. (2), (3) and (5) we calculated  $v$  of formic acid for each component. Table 3 summarizes the  $v$  values. Eq. (5) gives the most favorable value to the prepared one and Eqs. (2) and (3) give the larger one than the prepared value. Then, we can conclude that Eq. (5) gives the most relevant  $v$  value among the three equations. Eq. (4) may be applicable when we can observe  $T_{f(s)}$ .

#### 4.2. Concentration of $n$ -alcohols and polyethyleneglycol (PEG)

Fig. 3 shows the dependence of  $v$  evaluated by putting the peak temperature of  $\tan \delta$  (Manabe & Fujioka, 1998b;

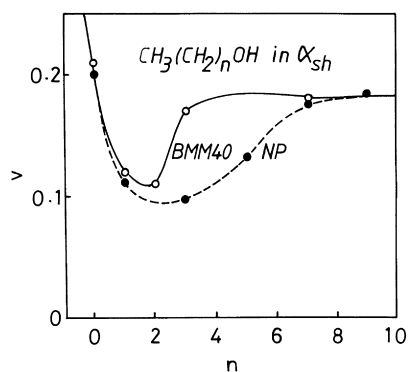


Fig. 4. Comparison between BMM40 and NP for  $v$  of  $n$ -alcohol in  $\alpha_{sh}$  region.

Manabe et al., 1986) into Eq. (5) on the numbers of carbon atoms,  $n$ , in chemical formula. Here, the chemical formula of  $n$ -alcohol is expressed by  $\text{CH}_3(\text{CH}_2)_n\text{OH}$  and one of PEG by  $\text{HO}(\text{C}_2\text{H}_4\text{O})_n\text{C}_2\text{H}_4\text{OH}$ . The  $v$  values given by open circles indicate the solvent concentration expressed by volume fraction in the region where the segments give rise to  $\alpha_{sh}$  absorption. The region corresponds to the interfacial area of a primary particle and is expressed as  $\alpha_{sh}$  region hereafter. The open and filled triangles stand for the  $v$  values relating to  $\alpha_{22}$  ( $\alpha_{21}$  region) and  $\alpha_{21}$  ( $\alpha_{21}$  region) absorptions, respectively. Both absorptions were originated by the segments existing in an inside of a primary particle. Fig. 3 indicates that (1) with an increase in  $n$ , the  $v$  values of  $\alpha_{22}$ ,  $\alpha_{21}$  and  $\alpha_1$  regions decreased monotonously and  $v$  showed a minimum at  $n = 2$  in  $n$ -alcohol for  $\alpha_{sh}$  region; (2) when the molecular weight, MW, was similar for  $n$ -alcohol and PEG,  $v$  of  $n$ -alcohol was larger than that of PEG for  $\alpha_{sh}$  region, on the other hand, for  $\alpha_{22}$ ,  $\alpha_{21}$  and  $\alpha_1$  regions the  $v$  values of  $n$ -alcohol were smaller.

Fig. 4 shows the comparison between BMM40 and NP for the value of  $v$  of  $n$ -alcohol in  $\alpha_{sh}$  region. If the diffusion of a solvent into  $\alpha_{sh}$  region is complete and the absorption equilibrium is attained, then, the  $v$  values of BMM40 and NP should coincide with each other. On the other hand, the results shown in Fig. 4 indicate that the  $v$  value of BMM40 is larger than that of NP in the case of  $n$ -alcohols with  $n$  ranging between 0 and 6, especially,  $n = 3$  (that is,  $n$ -butyl alcohol). In the case of NP, the diffusion of  $n$ -butyl alcohol was not enough for attaining the absorption equilibrium at 303 K within the immersing period of 48 h. Fig. 5 shows the dependence of  $E'$  and  $\tan \delta$  at 303 K on  $n$  in  $\text{CH}_3(\text{CH}_2)_n\text{OH}$  for NP swelled with  $n$ -alcohol.  $E'$  shows a maximum and  $\tan \delta$  a minimum at  $n = 3$  indicating that a cellulose solid in  $n$ -butyl alcohol could not sufficiently be plasticized comparing with other  $n$ -alcohols due to the low concentration of a solvent in  $\alpha_{sh}$  region. In the case of  $n = -1$  ( $\text{H}_2\text{O}$ ) and  $n = 0$  (methanol),  $E'$  is less than that after  $\alpha_{sh}$  absorption and these solvents diffuse into  $\alpha_{22}$  region, not only into  $\alpha_{sh}$  region.

#### 4.3. Solvent concentration $v$ in specified amorphous region

Fig. 6 shows the temperature dependencies of  $E'$  and  $\tan \delta$  for BMM40 immersed in  $\text{H}_3\text{C}-\text{OH}$ ,  $(\text{CH}_3)_2\text{CH}-\text{OH}$ ,  $(\text{CH}_3)_2\text{CH}_2-\text{OH}$ , and  $(\text{CH}_3)_3\text{C}-\text{OH}$ . The sharp peak of  $\tan \delta$  due to the melting of the solvent was observed from 10 to 30° lower than its melting point in bulk. The melting temperature depression has been observed for the case of water (Manabe & Fujioka, 1996), and the degree of the depression could be explained by the capillary condensation. By the use of the  $E'$  value after the melting, we can evaluate roughly the temperature location of a specified dynamic absorption. Table 4 summarizes the relationship between  $E'$  value and absorption. The temperatures of  $\beta_{a1}$  and  $\beta_{a2}$  absorptions for cases other than methanol locate near 260 and 210 K, respectively, and are higher than

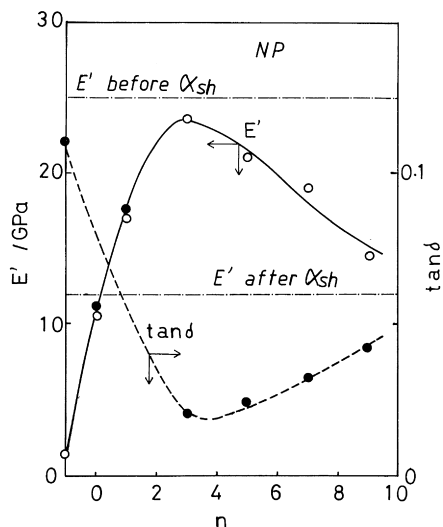


Fig. 5. Dependence of  $E'$  and  $\tan \delta$  at 303 K on  $n$  in  $\text{CH}_3(\text{CH}_2)_n\text{OH}$  for NP.

those in dry air. In the case of methanol,  $\beta_{a1}$  locates at 229 K and  $\beta_{a2}$  at 198 K.  $T_{fc}$  was determined and the  $\nu$  value was calculated by putting  $T_{fc}$  into Eq. (5). Table 5 summarizes the calculated  $\nu$  value. We can conclude the results of Fig. 6 and Table 5 as follows:

1. The  $\nu$  value in  $\alpha_{sh}$  region is influenced considerably by the group connecting to the carbon atom having an OH group. The  $\nu$  value shows a minimum at ethyl alcohol.
2. The  $\nu$  value to  $\alpha_{22}$ ,  $\alpha_{21}$  and  $\alpha_1$  regions indicate that  $\nu$  tends to decrease with an increase in molecular weight MW. When MW of solvents is similar to each other, the  $\nu$  for a tertiary alcohol is larger than others.

Fig. 7 shows the temperature dependence of  $E'$  and  $\tan \delta$  for BMM40 measured in the solvent represented by

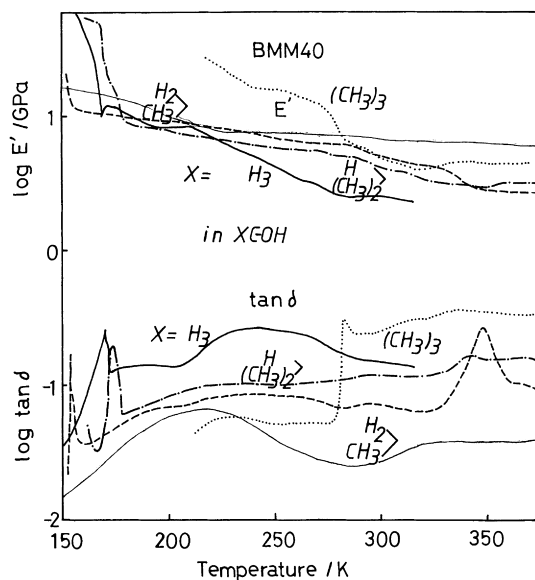


Fig. 6. Temperature dependence of  $E'$  and  $\tan \delta$  for BMM40 immersed in  $\text{H}_3\text{C}-\text{OH}$ ,  $(\text{CH}_3)_2\text{H}_2\text{C}-\text{OH}$ ,  $(\text{CH}_3)_2\text{HC}-\text{OH}$  and  $(\text{CH}_3)_3\text{C}-\text{OH}$ .

Table 4

Change in  $E'$  due to various dynamic absorptions for BMM40 and NP

| Dynamic absorption | Before or after | $E'$ (GPa)   |                       |
|--------------------|-----------------|--------------|-----------------------|
|                    |                 | BMM40        | NP                    |
| $\beta_{a1}$       | Before          | 20           | > 40                  |
|                    | After           | <sup>a</sup> | <sup>a</sup>          |
| $\beta_{a2}$       | After           | 8            | 24                    |
| $\alpha_{sh}$      | After           | 4            | 11                    |
| $\alpha_{22}$      | After           | 3            | 7.4                   |
| $\alpha_{21}$      | After           | 0.6          | 4.5                   |
| $\alpha_1$         | After           | 0.1          | 3.0, 2.0 <sup>b</sup> |

<sup>a</sup> Could not be determined.

<sup>b</sup>  $\alpha_1$  absorption tends to separate into two absorptions due to coexistence of a solvent.

$\text{XCHX}'\text{OH}$  (X and X' are hydrocarbon groups). The sharp peak of  $\tan \delta$  caused by the melting of the solvent is observed. The temperature is 10–30° lower than that of the solvent in a bulk. The  $\nu$  values are calculated by putting the observed  $T_{fc}$  into Eq. (5) and are summarized in Table 5. Here, the  $T_{fc}$  value was defined as the average between the two  $\alpha_{sh}$  absorptions separated. The  $\nu$  value for the  $\alpha_{sh}$  region is nearly independent of the existence of carbon atoms in X and X'. When the size of the lipophilic groups in X and X' increases in the solvents having similar chemical structure, the  $\nu$  value of  $\alpha_{sh}$  region increases. The  $\nu$  value of  $\alpha_{22}$  region increases with a decrease in MW and with a decrease in molecular weight per OH group in a molecule.

Fig. 8 shows the temperature dependence of  $E'$  and  $\tan \delta$  for NP immersed in the solvent expressed by  $\text{X}-\text{OC}_2\text{H}_4\text{OH}$  in a chemical formula (X; variable group). The peak temperature of  $\tan \delta$  is put into Eq. (5) and  $\nu$  is evaluated. The results are summarized in Table 5. Table 5 and Fig. 8

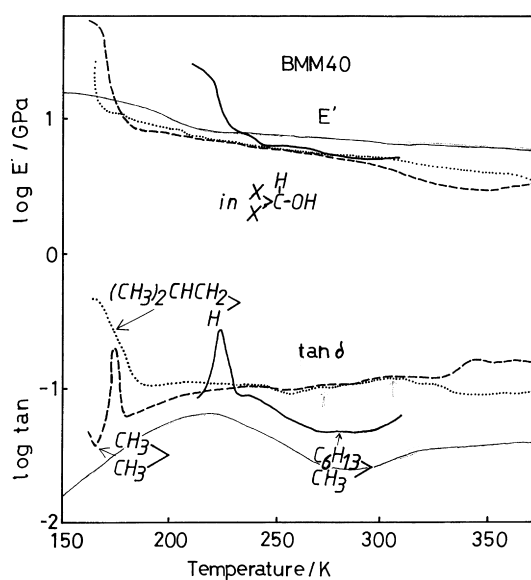


Fig. 7. Temperature dependence of  $E'$  and  $\tan \delta$  for BMM40 immersed in solvents represented by  $\text{XCHX}'\text{OH}$ .

Table 5

Solvent concentration  $\nu$  in a specified amorphous region for two cuprammonium regenerated cellulose BMM40 and NP

| Solvent chemical formula                                                | Regenerated cellulose sample | $\nu$         |               |               |            |
|-------------------------------------------------------------------------|------------------------------|---------------|---------------|---------------|------------|
|                                                                         |                              | $\alpha_{sh}$ | $\alpha_{22}$ | $\alpha_{21}$ | $\alpha_1$ |
| X-COH                                                                   | BMM40                        |               |               |               |            |
| X = H <sub>3</sub>                                                      |                              | 0.21          | 0.18          | 0.16          | < 0.11     |
| X = CH <sub>3</sub> H <sub>2</sub>                                      |                              | 0.12          | 0.085         | < 0.085       | < 0.085    |
| X = (CH <sub>3</sub> ) <sub>2</sub> H                                   |                              | 0.17          | 0.11          | < 0.080       | < 0.080    |
| X = (CH <sub>3</sub> ) <sub>3</sub>                                     |                              | 0.30          | < 0.21        | < 0.21        | < 0.21     |
| X-X'-CHOH                                                               | BMM40                        |               |               |               |            |
| X = CH <sub>3</sub> X' = CH <sub>3</sub>                                |                              | 0.16          | 0.11          | < 0.085       | < 0.085    |
| X = CH <sub>3</sub> X' = C <sub>6</sub> H <sub>13</sub>                 |                              | 0.20          | < 0.14        | < 0.14        | < 0.14     |
| X = H X' = CH <sub>3</sub>                                              |                              | 0.12          | 0.085         | < 0.085       | < 0.085    |
| X = H X' = (CH <sub>3</sub> ) <sub>2</sub> CHCH <sub>2</sub>            |                              | 0.13          | 0.062         | < 0.063       | < 0.063    |
| X-OC <sub>2</sub> H <sub>4</sub> OH                                     | NP                           |               |               |               |            |
| X = H                                                                   |                              | > 0.22        | 0.21          | 0.16          | 0.11       |
| X = C <sub>2</sub> H <sub>5</sub>                                       |                              | 0.21          | 0.13          | < 0.047       | < 0.047    |
| X = C <sub>2</sub> H <sub>4</sub> OH                                    |                              | 0.21          | 0.11          | 0.091         | 0.093      |
| X = C <sub>6</sub> H <sub>5</sub>                                       |                              | > 0.21        | 0.057         | 0.031         | < 0.031    |
| X = C <sub>2</sub> H <sub>4</sub> OC <sub>2</sub> H <sub>5</sub>        | NP                           | 0.061         | < 0.010       | < 0.010       | < 0.010    |
| X = C <sub>2</sub> H <sub>4</sub> OC <sub>2</sub> H <sub>4</sub> OH     |                              | 0.11          | 0.046         | 0.062         | 0.056      |
| HOCH <sub>2</sub> CH <sub>2</sub> -X-CH <sub>2</sub> CH <sub>2</sub> OH |                              |               |               |               |            |
| X = O                                                                   |                              | 0.21          | 0.11          | 0.090         | 0.065      |
| X = S                                                                   |                              | 0.17          | 0.080         | 0.088         | 0.079      |
| X = NH                                                                  |                              | 0.25          | 0.14          | 0.13          | 0.11       |

lead to the following conclusions: (1) with an increase in MW, the values of  $\nu$  in  $\alpha_{sh}$ ,  $\alpha_{22}$ ,  $\alpha_{21}$  and  $\alpha_1$  regions decrease for the case that X contains OH group; (2) when the molecular length increases all the  $\nu$  values in above amorphous regions decrease for the solvent with no OH group in X; (3) the smaller the molecular weight per OH group in a molecule, the larger the  $\nu$  values relating to  $\alpha_{21}$ ,  $\alpha_{22}$  and  $\alpha_1$  regions.

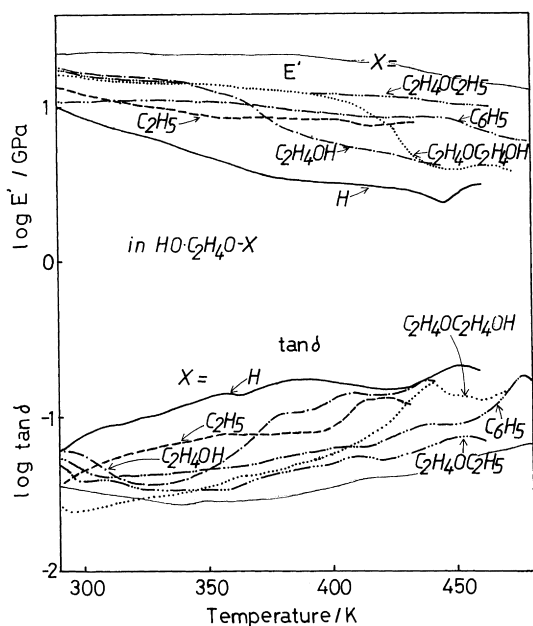


Fig. 8. Temperature dependence of  $E'$  and  $\tan \delta$  for NP immersed in solvents represented by X-OC<sub>2</sub>H<sub>4</sub>OH.

Fig. 9 shows the  $E'$  and  $\tan \delta$  vs. temperature curves for NP immersed in the solvent expressed by HOC<sub>2</sub>H<sub>4</sub>-X-C<sub>2</sub>H<sub>4</sub>OH. Here, X stands for S, O or NH. The case of glycerine as a solvent is also added as the solvent having three OH groups. As for the solvents with X = NH and S including glycerine,  $E'$  decreases sharply at 370 and 410 K. This steep gradient in  $E'$  may be originated from the acceleration of solvent diffusion into  $\alpha_{21}$  region due to the temperature

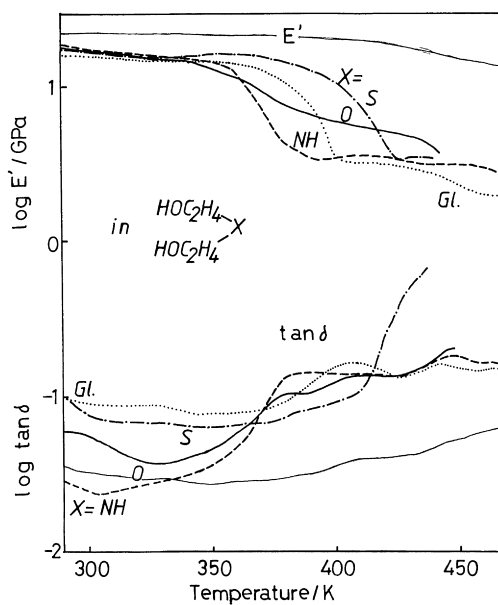


Fig. 9. Temperature dependence of  $E'$  and  $\tan \delta$  for NP immersed in solvents represented by HOC<sub>2</sub>H<sub>4</sub>-X-C<sub>2</sub>H<sub>4</sub>OH and glycerine.

elevation as was confirmed in glycerine (Manabe & Fujioka, 1998b). By putting  $T_{fc}$  into Eq. (5), the  $\nu$  value of each region is calculated and is summarized in Table 5. The  $\nu$  value of  $\alpha_{sh}$  region for the solvent with X of O or NH, which gives strong intermolecular hydrogen bond, is large. Especially, in the case of X = NH, the  $\nu$  values of all amorphous regions are always larger than those of other two solvents.

## 5. Conclusion

The solvent concentration  $\nu$  in a specified amorphous region was possible to be determined from the peak temperature of  $\tan \delta$  which was evaluated from the temperature dependence of dynamic viscoelasticities in a given solvent. The  $\nu$  value in  $\alpha_{sh}$  region was strongly influenced by the chemical structure of the solvent. The  $\nu$  values related to other amorphous regions were governed by the molecular weight per OH group in a solvent molecule.

## References

- Hatakeyama, T., & Kanetsuna, H. (1969). *Kobunshi Kagaku*, 26, 76.
- Haughton, P. M., & Sellen, D. B. (1973). *Journal of Physics D*, 6, 1998.
- Hermans, P. H. (1949). *Physical and chemistry of cellulose fibers* (pp. 220–226). Utrecht, Netherlands: Management of the A.K.U. and affiliated companies.
- Kamide, K., & Manabe, S. (1985). In D. R. Lloyd (Ed.), *Materials science of synthetic membrane*, (pp. 193). Washington, DC: American Chemical Society.
- Kamide, K., & Saito, M. (1985). *Polymer Journal*, 17, 919.
- Klotnikov, O. V., Mikhailov, A. K., & Rayavee, E. L. (1977). *Vysokomol. Soyedin. Ser. A*, 19, 2528.
- Kubat, J., & Pattyramie, P. (1967). *Nature*, 215, 390.
- Manabe, S., & Fujioka, R. (1996). *Polymer Journal*, 28, 860.
- Manabe, S., & Fujioka, R. (1998). *Third Micro-Symposium of the Cellulose Society of Japan*, (pp. 108). .
- Manabe, S., & Fujioka, R. (1998). *Polymer Journal*, 30, 939.
- Manabe, S., Iwata, M., & Kamide, K. (1986). *Polymer Journal*, 18, 1.
- Manabe, S., & Kamide, K. (1984). *Polymer Journal*, 16, 375.
- Manabe, S., Kamata, Y., Iijima, H., & Kamide, K. (1987). *Polymer Journal*, 19, 391.
- Manabe, S., Kamide, K., Nakayama, C., Kobayashi, S., & Text, J. (1977). *Machine Society of Japan*, 30, T85.
- Nakamura, K. (1956). *Kobunshi Kagaku*, 13, 47.
- Nakamura, K. (1957). *Kobunshi Kagaku*, 14, 544.
- Ramiah, M. V., & Goring, D. A. I. (1965). *Journal of Polymer Science C*, 11, 27.
- Simha, R., & Boyer, R. F. (1962). *Journal of Chemical Physics*, 37, 1003.
- Takayanagi, M., Harima, H., & Iwata, Y. (1963). *Memoirs of the Faculty of Engineering, Kyusyu University*, 23, 1.
- Tsurumi, T., Osawa, N., Hirasaki, T., Yamaguchi, K., Manabe, S., & Yamashiki, T. (1990). *Polymer Journal*, 22, 304.
- Webba, M., & Asiz, K. (1962). *Journal of Textural Institute*, 53, 291.